MASTER THESIS

FREQUENCY MODULATION IN ACOUSTICS AND PHOTOACOUSTICS

Sytze J. Bakker

BIOMEDICAL PHOTONIC IMAGING

EXAMINATION COMMITTEE
Prof. Dr. S. Manohar
M. Dantuma, MSc.
Prof. Dr. M. Versluis

06-11-2018

UNIVERSITY OF TWENTE.

Samenvatting

Voordat Photoakoestische tomografie een competitieve beeldvormings methode kan worden in het gebruik van borstkanker diagnose, moet er een verbetering worden doorgevoerd in de beelddiepte die bereikt kan worden. Dit wordt geprobeerd door het toepassen van technieken uit radar en communicatie wetenschappen. De techniek die is onderzocht in zijn effect in akoestische en photoakoestische(PA) fenomenen is het micro-Doppler photoakoestisch(mDPA) effect.

Uit de literatuur is de implementatie van het micro-Doppler photoakoestisch effect gehaald. Om de effecten van het mDPA effect op akoestiek en photoakoestiek zijn twee experimenten ontwikkeld. De vindingen uit deze experiment hebben alleen wetenschappelijke waarde in een fractie van de mogelijke configuraties van deze experimenten als gevolg van slechte verticale resolutie en het lineaire regime voor de initiële druk van de PA signalen die geproduceerd worden door laser licht belichting.

Na het uitvoeren van kalibratie metingen van de initiële druk van de PA signalen, bleek dat de data analyse alleen werkt in het geval dat het fantoom is gemaakt van ethanol en de laser puls energie 5 of 10 mJ is.

Het uiteindelijke resultaat van deze thesis is dat het mDPA effect niet de verbetering levert voor het PA signaal die was verwacht op basis van de literatuur, maar wat wel is gevonden dat het zeer waarschijnlijk is dat frequentie modulatie van een ultrasoon signaal mogelijk is als gevolg het photoakoestisch effect

Summary

For photoacoustic tomography(PAT) to become a competitive imaging modality in breast cancer diagnostics, the imaging depth needs to be improved. This is attempted by appropriating techniques from radar and communication science to improve signal quality over a longer distance. The main technique that was assessed for its effect in acoustic and photoacoustic(PA) phenomenon is the micro-Doppler photoacoustic(mDPA) effect

From literature the implementation of the mDPA effect was found. To find the effects of the mDPA effect on acoustics and photoacoustics two experiments were developed. For these findings to have scientific value it turned out that only a fraction of the experiments had value because the oscilloscope that was used was limited in its vertical resolution. Furthermore the initial pressures of the PA pulses have to fall in the linear regime for the data analysis to be valid, which further reduces the number of possible experimental configurations.

After performing calibration measurements of the pressures that are produced during laser light illumination, it was found that ethanol could be used as PA absorber with laser pulse energies of 5 and 10 mJ.

The final result of the thesis is that the mDPA effect does not provide the improvement in signal quality of the PA signal that was proclaimed in the literature, but that it is in most likely possible to frequency modulate an ultrasound signal using the photoacoustic effect.

Preface

Dear reader,

For this master thesis I have been working from November 2017 till November 2018 in the BMPI group at University Twente. During my time there I had some struggles maintaining my productivity at times. The time spent working on this thesis has solidified my desire to pursue becoming a physics educator, not becoming a researcher.

To get to this end result I have to first thank my supervisors Maura Dantuma and Srirang Manohar for their help. Other people that I have to thank for their help are Johan van Hespen, David Thompson and Guillaume Lajoinie. Also I would like to thank the students of ZH 268 that made this last year a lot of fun.

Sytze Bakker
Assen, 6 November 2018

Table of contens

Chapter 1. Introduction

1.1 Thesis introduction

The current medical diagnostic imaging devices market is dominated by a few companies.[1] This leads to monopolies for different types of devices for different companies, one manufacturer might dominate x-ray mammography while another controls a large market share for high field MRI scanners. The monopoly powers of these companies allow for them to set prices that maximize the profits for the companies while ignoring the societal cost and social costs these profits may induce.

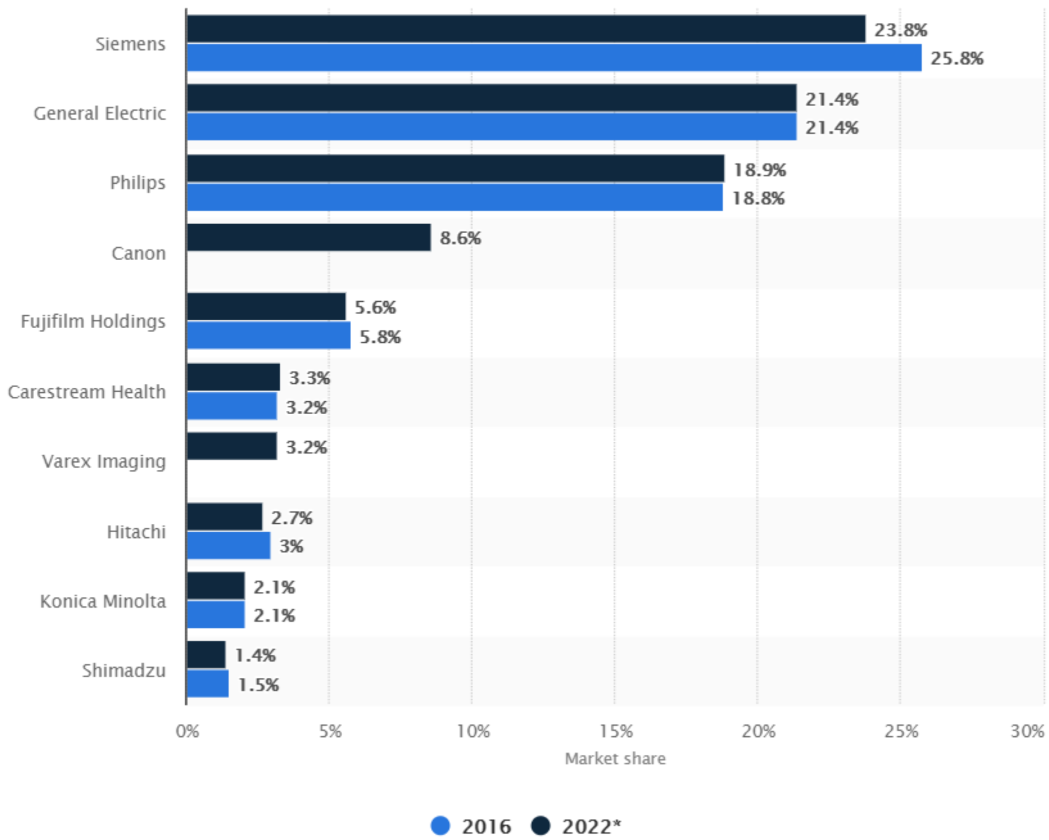

Figure 1 Shows the distribution of market share in the diagnostic imaging devices market in 2016, and a prognosis of expected market shares in 2022.[1]

The high pricing of the diagnostic imaging devices is a factor in the worldwide explosion of medical expenses, making medical expenses the leading cause of bankruptcy in the USA.[2] The methods that might help reduce the costs of these medical devices are by introducing increased competition, or direct government intervention in the market. Increased competition can be created through government regulation, like anti-trust policy, or through the introduction of new competitors by advancements in other technologies. In the current political climate large scale government intervention in the so called 'free market' is unlikely[3]. Increased government regulation also is unlikely as stringent anti-trust policy hardly has been enforced in decades[4]. Therefore In the field of biomedical engineering the introduction of new devices based on new technology seems to be the most obvious direction to pursue. There are a number of new imaging modalities that have been introduced in academic journals the last few years.[5-7] Of the newly introduced imaging techniques photoacoustic tomography is an opportune choice for imaging of the breast.[8] The breast is an area of the body that is currently imaged quite often as yearly 1.5 million women are impacted by breast cancer.[9] Since breast cancer is a disease that impacts so many women the desire for better and earlier detection of the disease may help overcome the barriers to entry that characterize a monopolistic market segment.[10-12]

PAT images the vasculature inside the breast. Since tumours contain higher blood vessel densities, they can be distinguished from healthy tissue. To bring PAT devices to market in the near future there are some issues that need to be solved. One of these issues is the imaging depth, which is limited to approximately 4 cm, and should be increased to make PAT suitable for breast cancer screening and diagnosis.[13] To accomplish a higher imaging depth, a method to increase the signal to noise ratio (SNR) of the signal is required.

In this thesis we investigate the applicability of methods used in radar and communication science in Photoacoustic(PA) imaging. When looking at radio signals the best SNR is accomplished by using frequency modulation (FM) of the system as opposed to amplitude modulation (AM).[14] Therefore it is a compelling direction for research to improve the PAT systems. In a paper by Gao et al. a method for creating FM signals using the photoacoustic effect was proposed, in conjunction with data that indicates the possibility of FM signal creation using the photoacoustic effect.[15] It is therefore worth exploring the applicability of using FM signal creation in improving the quality of photoacoustic signals. In this thesis this is done through first testing FM signal creation in a purely acoustic manner, then the photoacoustic case is tested.

1.2 Objective

The goal of this thesis is to determine the feasibility of using FM to improve the quality of PA imaging. The question that has to be answered to make such a determination is the following:

- Does the application of an exogenous ultrasound signal allow for improved quality of PA imaging using the micro-Doppler PA method?

This research question is divided into the following sub questions:
- Can Doppler shifts be detected from oscillating acoustic reflectors, oscillating at similar frequencies as the carrier wave?
- Is the mDPA effect proposed by F.Gao reproducible?
- Does the mDPA method induce frequency modulation in an exogenous ultrasound field?

1.3 Thesis structure

This thesis is constructed to find the effects of frequency modulation using the oscillating surface of an ultrasound transducer and photoacoustic source. In chapter 2 the theoretical background is explained. Chapter 3 introduces the experiments that were performed together with the additional insights that were necessary to perform the experiments correctly. Chapter 4 shows the results of the experiments that were introduced in chapter 3. Chapter 5 is a reflection on the steps that were taken to get the results of chapter 4 and the conclusions that can be drawn from those, with an outlook into the viability of applying any of the findings of the thesis in any future research or application.

Chapter 2. Theoretical background

2.1 Introduction

In order to understand the method that F. Gao et al used to modulate the photoacoustic signal, knowledge about acoustics is required. This chapter explains the physics behind relevant elements of photoacoustics and acoustic wave propagation after which the theory from the above mentioned paper is introduced.

2.2 Acoustic wave propagation

Acoustic wave propagation describes the behaviour of sound waves. In this case the area of interest is the ultrasound domain. Ultrasound covers the domain of sound that falls outside the upper limit of human hearing which is approximately 20 kilohertz. The propagation of acoustic waves is defined by the acoustic wave equation as shown in equation 3. This is the linear acoustic wave equation in three dimensions[16].

$$\nabla^2 p - \frac{1}{c^2}\frac{\partial^2 p}{\partial t^2} = 0 \tag{1}$$

Where p is the pressure in Pascal and c the speed of sound. While propagating, the sound wave loses some of its energy by two major types of propagation losses. These are geometric spreading losses and absorption losses. Geometric spreading loss is defined as the propagation of acoustic waves from a sound source where the waves propagate towards a larger and larger area. As energy is conserved and assuming energy is not converted into another type of energy, the intensity (proportional to pressure squared) is inversely proportional to the surface the wave covers. The simplest case is that of a point source in an infinite homogenous medium radiating in all directions.[17]

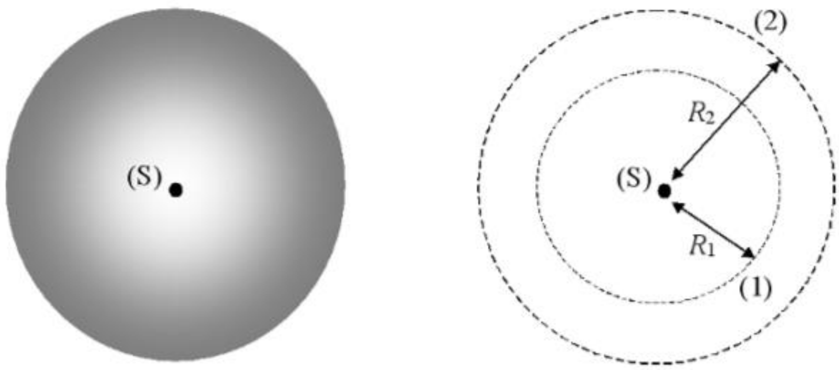

Figure 2 Illustration of an acoustic point source.[17]

So the relation of the intensity between points (1) and (2) is inversely proportional to the surfaces of the spheres that correspond to the respective radii:

$$\frac{I_2}{I_1} = \frac{\Sigma_1}{\Sigma_2} = \frac{4\pi R_1^2}{4\pi R_2^2} = \left(\frac{R_1}{R_2}\right)^2 \tag{2}$$

The medium absorbs a part of the transmitted wave energy, which is dissipated through viscosity i.e. heat generation. For an acoustic plane wave the acoustic amplitude decreases exponentially with distance.[18] As is shown by equation 3.

$$A(x,t) = A_0 \exp(-\alpha x) \exp\left[i\omega_c \left(t - \frac{x}{c_0}\right)\right] \tag{3}$$

Where A_0 is the initial amplitude, α is the attenuation coefficient, ω_c is the frequency of the wave and c_0 is the speed of sound. Also higher frequencies attenuate faster than lower frequencies.[19] This can be expressed through an attenuation coefficient α in decibels per meter per mega Hertz (dB/m/MHz).[19] Where the attenuation coefficient is expressed by equation 4, showing the dependence of the attenuation on the frequency.

$$\alpha(f) = \alpha_0 + \alpha_1 |f|^y \tag{4}$$

Where α_0 is often zero and y is a power law exponent and generally one.[19]

So for a complete analysis of the losses in photoacoustic pressure the dilution through geometric spreading and the losses through attenuation need to be multiplied to give the full answer. In this thesis the experiment will be performed in a water tank at short distances, so the attenuation can be ignored[19].

2.3 Photoacoustics

The photoacoustic effect was discovered by Alexander Graham Bell,[20] who found that an acoustic signal was produced when a sample in an enclosed cell is illuminated with light having a periodically varying intensity. Subsequent work showed that this “photoacoustic effect” also occurred with liquid and gas samples.[21]

2.3.1 The pulsed effect

The pulsed photoacoustic effect is a thermoelastic expansion process that results in an acoustic wave. The thermoelastic expansion is induced by the absorption of laser light.[22] To effectively produce an acoustic wave there are some requirements that need to be fulfilled.[23] The first is that the thermal diffusion shouldn’t be able to dissipate the heat, to be sure this does not occur the pulse duration should meet the following condition $t_p < \frac{d^2}{\kappa}$

where t_p is the pulse duration, d is the size of the optical absorption zone and κ the thermal diffusivity.[24,25] The other requirement is that of stress confinement where the pressure accumulation should not be reduced as a result of stress waves, such that there is a maximum in terms of stress confinement. To meet this requirement the following should hold $t_p < \frac{d}{v_s}$ where t_p is pulse duration, d is the size of the optical absorption zone and v_s is the speed of sound.[24,25] This limit results in a maximum stress confinement in the optical absorption zone, which then allows for the thermoelastically induced pressure to reach the maximum.[25] This pressure will cause maximum stress fields that can then propagate as a stress wave beyond the confines of the optical absorption zone.

When the pulse duration is in accordance with both of these conditions the fractional volume expansion $\frac{\Delta V}{V}$ during the pulse can be neglected.[26] Resulting in equation 5.

$$\frac{\Delta V}{V} = -K\Delta p + \beta \Delta T = 0 \tag{5}$$

Where K is isothermal compressibility, β the coefficient of thermal expansion, Δp the change in pressure and ΔT the change in temperature. The change in pressure (Δp_0) through absorption can be written as.[27]

$$\Delta p_0 = \frac{\beta \Delta T}{K} = \frac{\beta}{K}\left\{\frac{E_a}{\rho C_v}\right\} . \tag{6}$$

With ρ the mass density, C_v the specific heat at constant volume, E_a the absorbed optical energy per unit volume given by the product of μ_a absorption coefficient and I the fluence at the local absorption point. This can be written as:

$$\Delta p_0 = \Gamma E_a \tag{7}$$

Where

$$\Gamma = \frac{\beta}{K\rho C_v} = \frac{\beta {v_s}^2}{C_p} \tag{8}$$

The term Γ is the Grüneisen coefficient, a parameter that combines the thermal expansion coefficient, the speed of sound and the compressibility. So the Grüneisen coefficient is a unitless material property that converts the absorbed energy into the initial pressure amplitude. The pressure distribution of a spherical absorber is given by equation 9.[28]

$$p(r,t) = \frac{1}{2}\sqrt{\frac{\pi}{2}}\frac{p_0}{r}[(r - v_s t)sgn\left(\frac{r+R}{v_s} - t\right) + (-r + v_s t)sgn\left(\frac{r-R}{v_s} - t\right) \tag{9}$$

Where R is the radius of the spherical absorber.

2.4 Micro-Doppler photoacoustic effect

In traditional radar, i.e. electromagnetic waves, objects are detected using the reflection of electromagnetic waves that are send by the radar system. If an object is moving at a certain speed, the carrier frequency of the returned signal will be shifted, i.e. the Doppler effect[29]. Where the shift of the frequency is given by equation 10.

$$\Delta f = f_c \frac{2\Delta v}{c} \tag{10}$$

Where Δf is the frequency shift, f_c is the carrier frequency, Δv is the difference in speed between source and observer and c is the speed of the wave propagation.
If the object possesses an additional mechanical vibration or a rotation, the carrier frequency might undergo another frequency modulation. This is called the micro-Doppler effect[30]. One example of this phenomenon is a helicopter as the bulk movement of a helicopter will shift the frequency of the carrier frequency as well as the rotors of the helicopter inducing an additional time varying doppler shift.

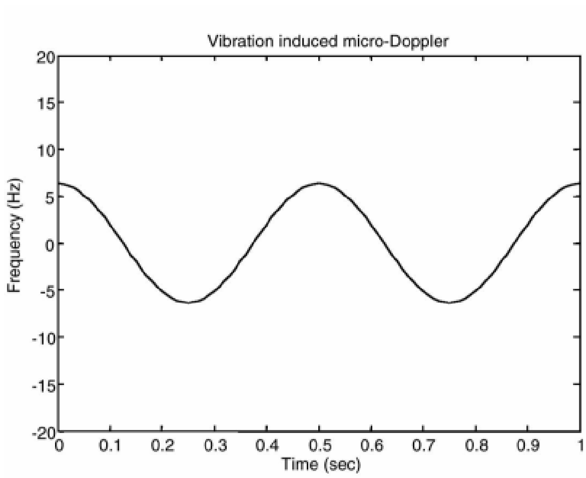

Figure 3. Shows the model that follows micro Doppler in radar for a vibrating surface. b) the result of the simulation of a radar set up as done by Chen et al.[30]

The frequency shift generated by an oscillating of the object is shown in figure 3 where the translation of the object is constant and the frequency difference is attributed to the vibration of the object surface.[30] Where a positive frequency shift indicates the object is moving towards the observer and a negative shift is when the object is moving away from the observer.

The micro-Doppler photoacoustic effect (mDPA) is a possible manifestation of this phenomenon to acoustic waves as micro-Doppler is to electromagnetic waves, since traditional Doppler also exhibits an acoustic variant that is based on the same underlying principle as the electromagnetic variation. The acoustic Doppler effect is used in biomedical devices to image flow in liquids.

F. Gao et al. were the first to apply this micro-Doppler effect onto a photoacoustic object, they used the micro-Doppler effect to create a frequency modulated signal (FM) that should retain a better signal to noise ratio opposed to the relatively weak photoacoustic signal that is generated.[15] The goal of the method is to improve the SNR of photoacoustic methods and as a result improving sensitivity and imaging depth.

The ultrasound functions as radar and the photoacoustic effect causes vibrations in the optical-absorbing object. The mDPA is accomplished by transmitting continuous wave (CW) bursts of ultrasound towards a photoacoustic arbsorber. The backscattering from the optical-absorbing object is received, covering the time interval where the absorber is excited by a pulsed laser. The photoacoustic effect induces a micro-doppler shift to the ultrasound wave over the length of the photoacoustic expansion. Since this frequency shift is different from the frequency shift obtained from bulk movement of the object it is attributed to the mDPA effect. F. Gao et al describe the Doppler shift the CW ultrasound experiences using a simplified model of the mDPA effect as is visible in figure 4, where a plane CW ultrasound wave with frequency f_0 hits a circular target with diameter R.[15]

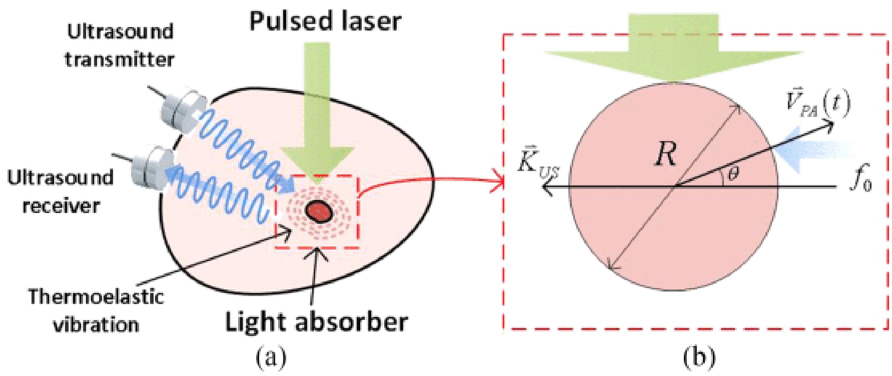

Figure 4. The mDPA effect and modelling. (a) Visual representation of the laser illumination in combination with an external ultrasound field. The mDPA effect occurs when the laser-induced thermoelastic vibration modulates the external ultrasound field. (b) Round-shape model where the absorber with radius R is illuminated from above and the ultrasound is coming from the right[15].

The transient velocity vector (V), describes the speed of the absorber's surface and is proportional to the derivative of the photoacoustic pressure $p(t)$ and can be expressed as:

$$V_{PA} = \kappa_s R \frac{\delta p(t)}{\delta t} \tag{11}$$

Where κ_s is the adiabatic compressibility. Then from equation 12 the doppler shift as a result of the expansion of the expansion of the absorber can be expressed. When taking into account the orientation of the ultrasound to the direction of the expansion, the transient micro-Doppler frequency shift can be expressed as:

$$f_{mDPA}(t) = 2f_0 \frac{V_{PA}(t)}{c} \cos\theta = \frac{2f_0 \kappa_s R}{c} \frac{\delta p(t)}{\delta t} \cos\theta \tag{12}$$

Where θ is the vibration angle as shown in figure 4. As equation 12 shows the frequency modulation of the mDPA effect is proportional to the derivative of the photoacoustic pressure, allowing for the photoacoustic information to be extracted from the mDPA data.

Based on the results obtained by F. Gao et al. the expected measured signal and the analyzed signal are shown in figure 5.

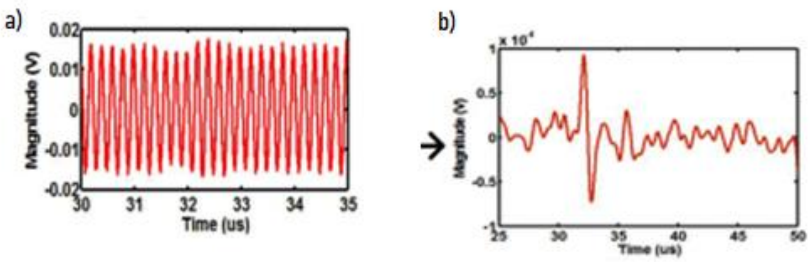

Figure 5 a) shows the signal as it was measured by F.Gao et al. in the temporal range where the pulse of the laser occurs in the signal. b) shows the result of the mDPA method and its analysis.[33]

2.5 Data analysis

F. Gao et al. have developed a data analysis method to find the modulation frequency of the reflected CW ultrasound signals as is previously described. They use a down conversion technique which mixes the reflected ultrasound signal. which enables the removal of the signal together with the photoacoustic signal such that that the mDPA remains. For the down conversion the received ultrasound signal $US(t) = A_{US}\sin[2\pi(f_0 + f_{mDPA})t]$ must be multiplied with a reference signal $R(t) = A_R\cos[2\pi f_0 t]$, with A_{US} A_R the respective amplitudes.

This results in the following equations:

$$D_{mixed} = US(t)\,R(t) \tag{13}$$

$$= A_{US}A_R \sin[2\pi(f_0 + f_{mDPA})t]\cos[2\pi f_0 t] \tag{14}$$

$$= \frac{1}{2}A_{US}A_R \sin[2\pi(\,2f_0 + f_{mDPA})t] + \frac{1}{2}A_{US}A_R \sin[2\pi\, f_{mDPA}t] \tag{15}$$

Due to the down conversion the frequency modulation of the original signal can be filtered more easily, since every part with a different frequency relative to the original signal will have a comparatively low frequency whereas the unmodulated parts will get twice their original frequency. Using a low pass filter the high frequency elements can be filtered away leaving only the modulated parts of the reflected signal. The result of low pass filtering is shown in equation 16.

$$mDPA(t) = \frac{1}{2} A_{US} A_R \sin[2\pi\, f_{mDPA} t] \tag{16}$$

It is important to use the correct cutoff frequency for the low pass filter.

Chapter 3. Materials and Methods

3.1 Introduction

To research the creation of frequency modulated signals using the oscillation of the surface of an acoustic source and a photoacoustic source, first an experiment where the acoustic source is an ultrasound transducer and the carrier wave is produced using a ultrasound transduce. Using the insight that is gained during such an experiment the parameters for the photoacoustic source can be determined. The inspiration for the experiments came from Mujica et al. and F.Gao et al. [15,29]

3.2 Experimentation micro-Doppler acoustics

3.2.1 Static Doppler effect

The model of the mDPA effect can be used to provide an expectation for the results that should be the outcome of this experiment. Using this approach the measurements can be compared to the expectation based on the mDPA or static Doppler effect.
The expectation that comes from the static Doppler effect is the same as for the mDPA effect, and is given by the following expression[29].

$$f_{mD}(t) = 2 f_0 \frac{V_t(t)}{c} \cos\theta \tag{17}$$

Where f_0 is the carrier frequency of the ultrasound radar system, c is the speed of sound of the medium, $V_t(t)$ is the velocity of the surface of the transducer. The velocity of the transducer system is given by:

$$V_t(t) = A_t \sin(\omega_t t) \tag{18}$$

A_t is the amplitude of the oscillation of the transducer surface, ω_t is the angular velocity corresponding to the 0.5 MHz drive frequency of the transducer. Since the transducers are oriented such that $\cos\theta$ equals 1 and can thus be ignored.
Using the data analysis procedure of chapter 2 the expected results for the measurements are given by the following equation:

$$mD(t) = \frac{1}{2} A_{US} A_R \sin[4\pi\, f_0 \frac{A_t \sin(\omega_t t)}{c} t] \tag{19}$$

The expectation for the experiment in case $A_{US} = 1,\ A_R = 1$ and $A_t = 1\mu m$ is given in figure 6.

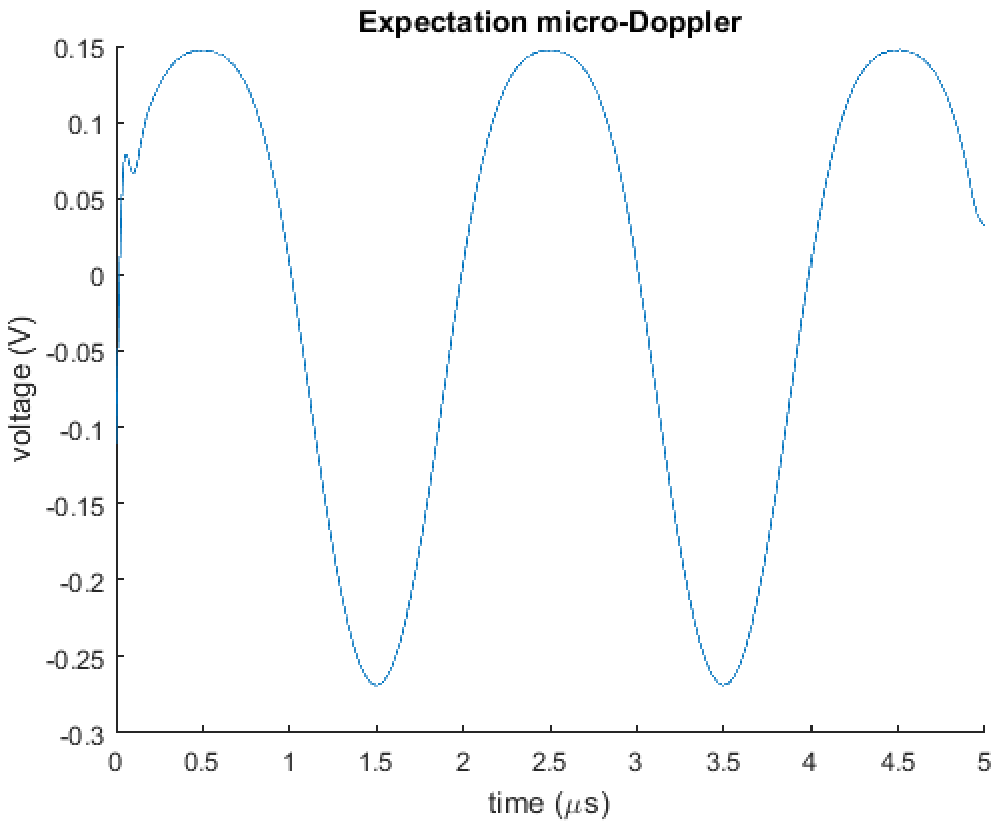

Figure 6. Simulation result of the outcome of a micro-Doppler experiment.

3.2.2 Quasistatic Doppler effect

In the quasistatic Doppler effect the effect of the oscillating surface on the carrier wave is given by $f_{mD} = f_0 \pm nF$ where F is the frequency of the oscillations and n is an integer number[29]. The total number of n that shows up in the signal is dependent on the strength of the oscillation, or in this case the amplitude of the movement. Therefore the signal that is received based on the quasistatic Doppler effect is given by:

$$mD(t) = \frac{1}{2} A_{US} A_R \sin[2\pi \, (f_0 \pm nF) \, t] \tag{20}$$

Since the cutoff frequency of the low pass filter in the data analysis is chosen to be 2 MHz the only n that are of influence in the experiment are up to n=4.

3.2.3 Experimental setup

The first constraint for the system is that the duration of a single period for the oscillating scatterer has to be longer than the period of the ultrasound signal that is used as the ultrasound radar system. Otherwise the effect of the frequency modulation will be confined within one period of the ultrasound signal making it harder to measure the frequency shift that is applied to the ultrasound signal. Since the frequency of the radar is known which is 5 MHz the transducer frequency is chosen to be 0.5 MHz. This should allow for the measurement of the Doppler shift of the signal using the data analysis of chapter 2. The set up that is used for this experiment is shown in figures 7 and 8.

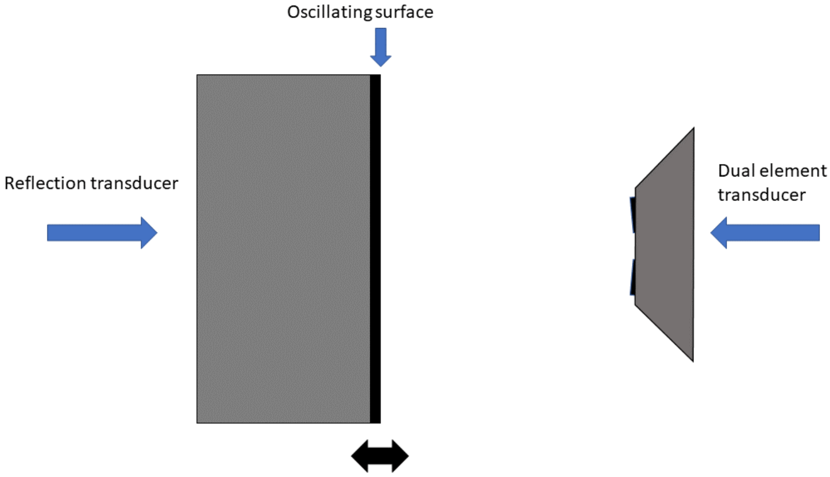

Figure 7. The set up for determining the process of frequency modulation.

Where figure 8 is the schematic of the system.

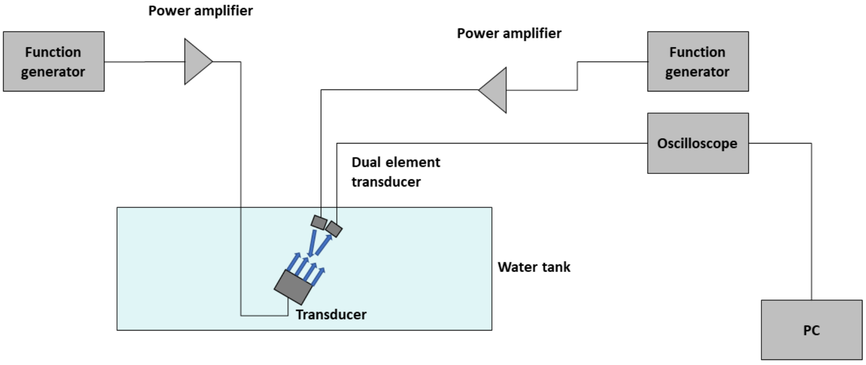

Figure 8. The schematic of the complete measurement set-up.

The transducers that were used were the 5 MHz dual element transducer DHC711-rm (Olympus), and the 0.5 MHz V389-SU (Panametrics). The spacing between the transducers is 3 cm. Also 2 power amplifiers were used to drive both of the transducer that are employed for the experiments.

Setting up the experiment is done by first aligning to two transducers to be parallel to each other. Then the radar element of the system of the system is turned on to check that the receive element of the dual element transducer is properly receiving a reflection coming from the surface of the 0.5 MHz transducer. A secondary control is to connect both the input of the send element and the output of the receive element to the oscilloscope where the delay between sending the ultrasound and receiving the signal with the receive element corresponds to the distance between the transducers. After that the reflection transducer is turned on to send out the 0.5 MHz signal. Finally the data acquisition is turned on to read out the oscilloscope. The data is read out using Matlab using some version of the script in appendix 1. The timing scheme for this experiment is given in figure 9.

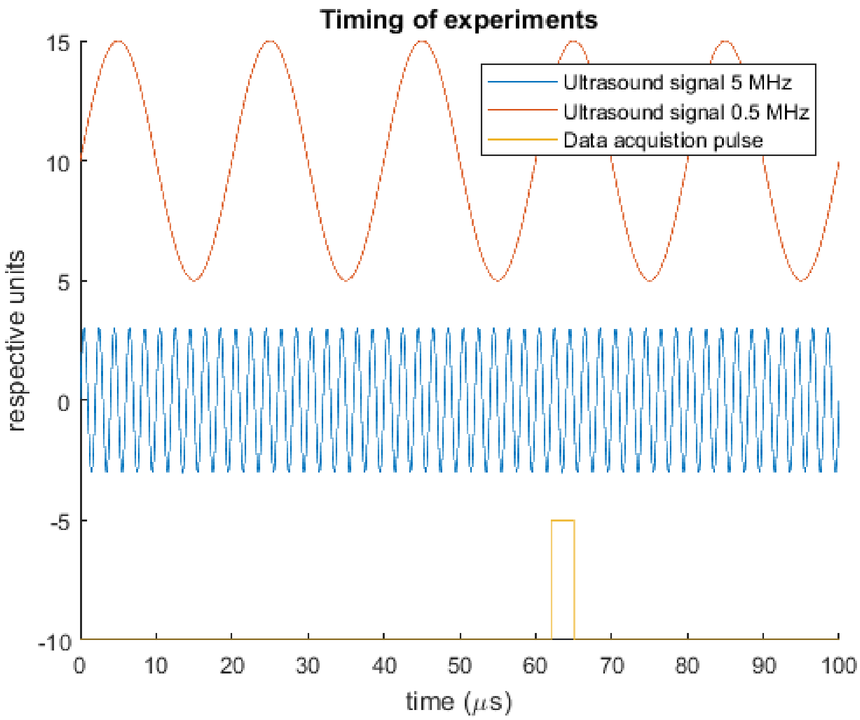

Figure 9. Timing scheme for micro-Doppler experiment.

3.2.3.1 Function generator

The function generator is programmed in its first channel to create a 5 MHz sine wave with a duration of 500 cycles with an amplitude of 100 mV peak to peak and this output is fed into the power amplifier. For the second channel a pulse of 0.5 MHz is created with a duration of 50 cycles where the peak to peak amplitude of the signal is dependent on the amplification of the power amplifier and the desired output voltage.

3.2.3.2 Oscilloscope

The oscilloscope is connected to the output of the receive element, and triggered by the output of channel 2 of the function generator. The triggering of the oscilloscope makes sure the laser pulse signal arrives at the transducer at 4 µs after the triggering starts and the timescale is 1 $\frac{\mu s}{div}$ and the voltage scale is 50 $\frac{mV}{div}$. This makes sure the pulse occurs in the middle of the window of the oscilloscope. Which can then be read out by the computer.

3.2.3.3 Power amplifier

The power amplifiers have a gain of 50 dB which means that the input voltage is amplified by a factor of 316. Using this amplification the output that is fed into the 5 Mhz transducer send element has a peak to peak voltage of 31.6 V.

3.3 Experimental set-up F. Gao et al.

First the set-up from F. Gao has to be analysed to determine the essential elements that are required for the detection of the mDPA effect, and the points of possible improvements can be assessed. The set-up of F. Gao et al. is shown in figure 10.

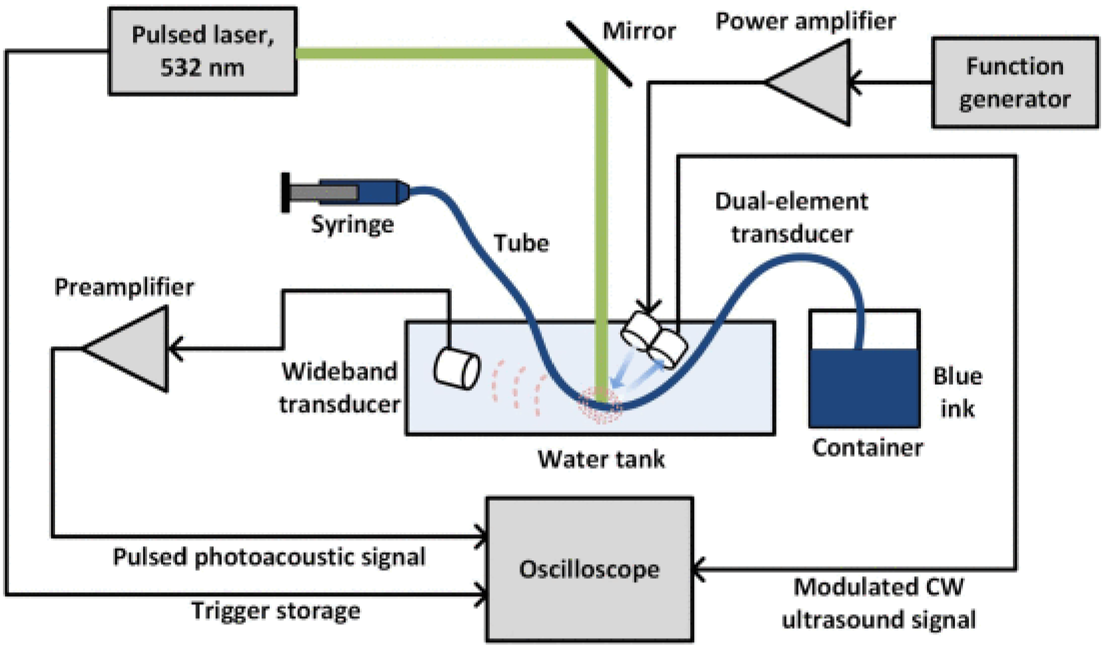

Figure 10 Schematic of set-up used by F. Gao et al. for their experiments.[15]

The set-up used by F. Gao et al. consists of a Q-switched Nd:YAG laser at 532nm emitting single laser pulses with 7 ns pulse width (Orion, New Wave, Inc.). The collimated laserbeam with 2 mm diameter spot size is guided onto a silicone tube immersed in water filled with diluted blue ink (Pelikan, $\mu_a \approx 10$ mm^{-1}) pumped by a syringe pump[15]. They use two ultrasound transducers. The first transducer (V323-SU, 2.25 MHz, 6 mm in diameter; Olympus) is used to act as a reference measurement to measure the PA signal conventionally. The second is a dual element transceiver, and is used by simultaneously running both elements of a dual-element transducer (5 MHz, 6 mm in diameter, DHC711-RM; Olympus) with one element in send and the other in receive mode[15]. This means that it operates as an ultrasound radar. Where a function generator is fed into a power amplifier to drive the send element. The receive element is connected to the oscilloscope. Both transducers are placed at a distance of 45 mm with respect to the tube. The data acquisition is triggered by a synchronization pulse from the laser[15].

3.4 Validating set-up photoacoustic source

3.4.1 Introducing planned set-up

Based on the elements that are presented the necessary components for the data acquisition are the dual element transducer, the function generator, the power amplifier, the pulsed laser and the oscilloscope. The main improvement that was thought of was the implementation of a lock-in amplifier to analyze the data directly as it is received. The function of a lock-in amplifier is the same as the data analysis that was provided in the paper by F.Gao et al. and described in equations 13-16. from chapter 2.

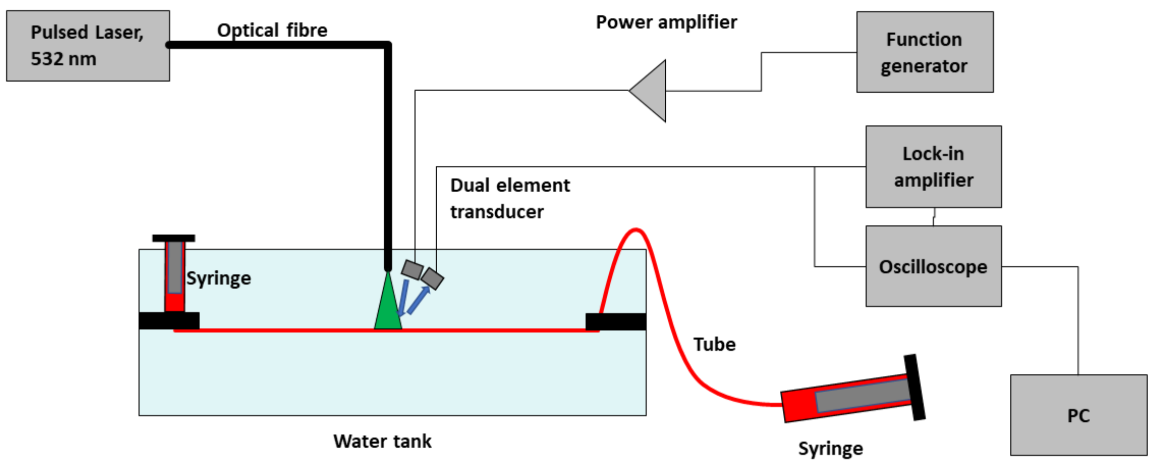

Figure 11 Schematic of the initial set-up plan.

A schematic representation if the planned experimental set-up is given in figure 11. The set-up consists of a Q-switched Nd:YAG (Quanta Ray Pro 250-10, Spectra-Physics) laser working at the 532 nm wavelength with a pulse width of 8-10 ns. The pulse width fulfils the requirements of thermal- and stress confinement. The laser is coupled into an optical fibre where the resulting spot size on the tube surface has a radius of 10 mm. The PTFE tube, with an inner diameter 0.5 mm and outer diameter is 0.67 mm, is connected at both ends to syringes where one syringe is filled with a red ink solution.. The other syringe is empty, this allows for the tube to be flushed after each set of experiments to prevent the deposition of residue inside the tube. The tube pulled to be under slight tension to make sure it is straight. to F. Gao et al. we have chosen to not use a secondary reference transducer but instead perform the experiment both in ultrasound radar mode as in receive mode with one element. So the only transceiver system that was used was a dual element transducer(DHC-711 rm, Olympus) with a centre frequency of 5 MHz and a 40% bandwidth. The function generator that was fed into the power amplifier (RF power amplifier A-075, electronics & innovation) was a Tektronix AF63102 function generator. The lock-in amplifier connected to the receive element is a HF2LI lock-in amplifier(Zurich instruments). For the alignment an oscilloscope(TPS2024B,Tektronix) is also attached to the receive element. So if the dual element transducer was operating in its ultrasound radar mode the optimal positioning of the transducer with respect to the tube can be found.

3.4.2 Testing usefulness of lock-in amplifier

To test the functionality of the lock-in amplifier in the planned set-up the output of the lock-in amplifier will be compared to a digital data analysis to see if there are no problems introduced in the detection of the mDPA effect as a result of the use of a lock-in amplifier.

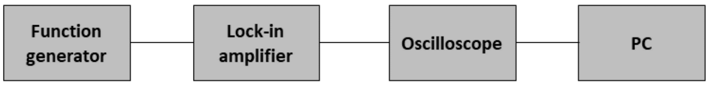

Figure 12 Schematic for testing the lock-in amplifier.

The measurement is performed by creating the following trial waves:

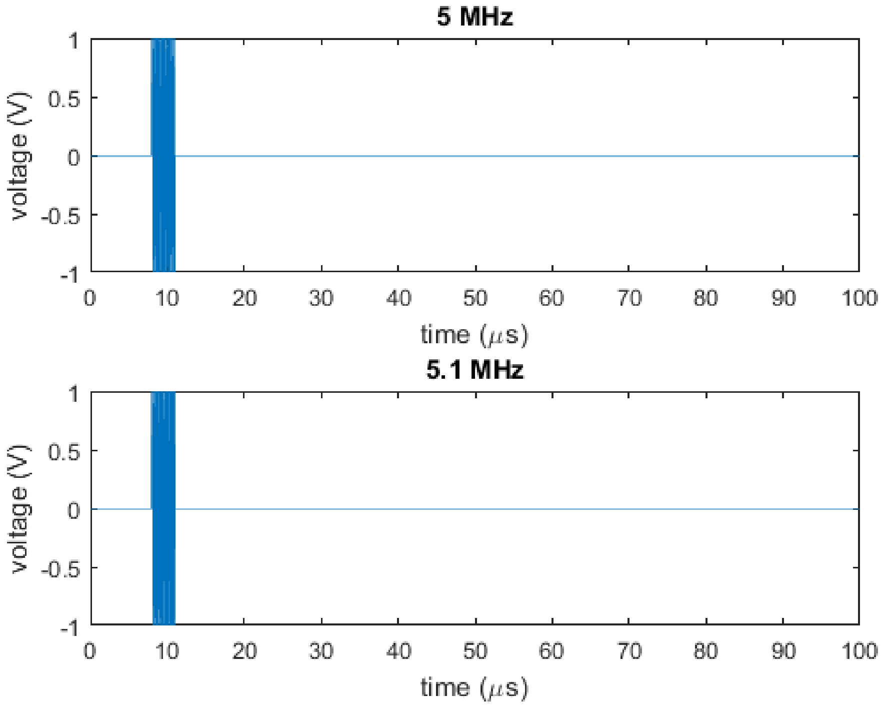

Figure 13 trial waves for testing the lock-in amplifier

These trial waves can then be analyzed by either the lock-in amplifier or the digital implementation of the data analysis of 2.5.

3.4.3 Experimental set-up mDPA

For the measurements of the mDPA experiments the usefulness of the lock-in amplifier turned out to be rather low. Therefore the decision was made to do the data analysis digitally. The results of the experiment in 3.4.2 is further explained in chapter 4. The receive element of the dual element transducer is therefore directly connected to the oscilloscope and the oscilloscope is read out by the PC using MATLAB, in the same way as for the . Since the data processing is done on a PC the reference signal can be produced on the PC. So the final set-up looks like figure 14.

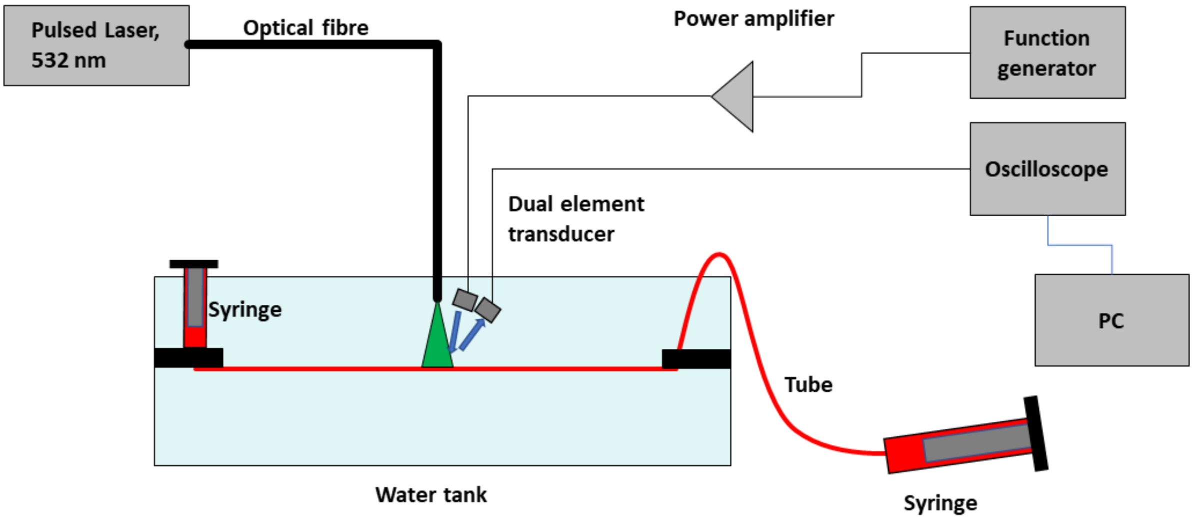

Figure 14 the final set-up used in the experiments.

The set-up is operated in the is operated in the same fashion as for the set-up of 3.2 with the addition of the laser. The set-up can be used as the ultrasound radar where both the send and receive element of the dual element transducer are turned on. The set-up can also be used to directly measure the produced PA signal when the send element is turned off, this gives the best comparable improvement in signal quality as the result of the mDPA effect.

3.4.3.1 Laser

The Quanta Ray Pro 250-10, Spectra-Physics is operated at 532 nm with a pulse width of 8-10 ns. For the experiments the laser energy per pulse is monitored, so the laser energies are consistent throughout the experiment. The spot size of the laser light has a diameter of 1 cm at the tube, which was measured using a protractor. The trigger output for the laser is connected to the external trigger input of the function generator.

3.4.4 Pressure of the photoacoustic pulses

The system of the calibration measurement differs from the set up for the mDPA effect in the sense that the dual element transducer is replaced by the calibrated hydrophone needle. This is represented in figure 15.

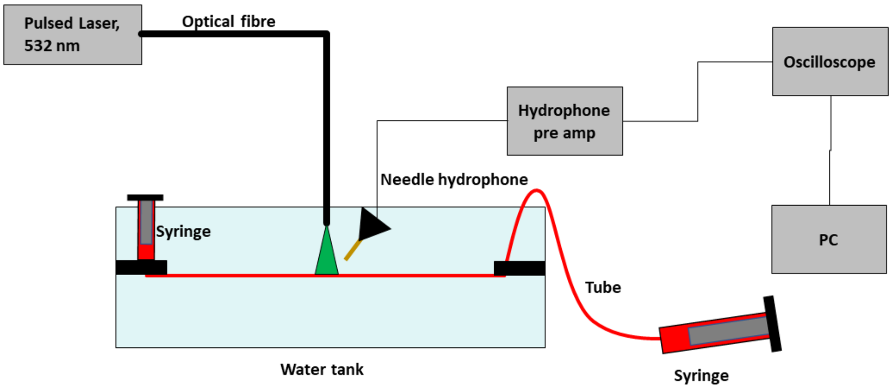

Figure 15. The set up for the calibration experiment.

The hydrophone system is a precision acoustics needle hydrophone with a 1 mm needle that is calibrated. Using this set up the calibration of the PA signal are performed for both the tube filled with water and red ink and the tube filled with ethanol and red ink, the same as for the set up in the previous paragraph. The pulse energies that are used are 5, 10, and 15 mJ per pulse with the same set up as for the mDPA measurement i.e. the positioning of the laser fiber and the tube is consistent across all the measurements. Except for the needle hydrophone that is placed on the position that was used for the dual element transducer

3.5 Revised mDPA experimentation

3.5.1 Additional system phenomena analysis

3.5.1.1 Photoacoustic pulse

The expansion of the model of the mDPA effect should be the photoacoustic pulse that is generated when the absorber is illuminated by the laser light. It has been shown that the photoacoustic pulse $p_{PA}(t)$, that is the pressure in Pa as a function of time, has reached the transducer with a measurable intensity[15]. The photoacoustic pulse can be assumed to behave like a set of harmonic oscillators with frequencies $\sum f_{PA}$.

$$p_{PA}(t) = A_{PA}\sin(2\pi \sum f_{PA}\, t) \tag{21}$$

Since the PA signal also reaches the transducer, the measured ultrasound signal can't be represented by $US(t) = A_{US}\sin[2\pi(f_0 + f_{mDPA})t]$, the basis of the data analysis in 2.5.as was assumed by F. Gao et al., but it must be represented by the following equation:

$$US(t) = A_{US}\sin[2\pi(f_0 + f_{mDPA}(t))t] + p_{PA}(t) \tag{22}$$

Following the same down conversion and filtering as is described in chapter 2, equations 13-16 will be replaced by equations 23-25.

$$mDPA(t) = [A_{US}\sin[2\pi(f_0 + f_{mDPA}(t))t] + A_{PA}\sin(2\pi \sum f_{PA}\, t)]A_R\cos[2\pi f_0 t] \tag{23}$$

$$mDPA(t) = \frac{1}{2}A_{US}A_R\sin[2\pi(\,2f_0 + f_{mDPA}(t))t] + \frac{1}{2}A_{US}A_R\sin[2\pi\, f_{mDPA}(t)t] + \frac{1}{2}A_R A_{PA}\sin\left(2\pi\left(\sum f_{PA} - f_0\right)t\right) + \frac{1}{2}A_R A_{PA}\sin\left(2\pi\left(\sum f_{PA} + f_0\right)t\right) \tag{24}$$

$$mDPA_{filtered}(t) = \frac{1}{2}A_{US}A_R\sin[2\pi\, f_{mDPA}(t))t] + \frac{1}{2}A_R A_{PA}\sin\left(2\pi\left(\sum f_{PA} - f_0\right)t\right) \tag{25}$$

The problem that becomes apparent when accounting for the frequency behaviour of photoacoustic pulses is that the pulses are not well defined single frequencies but instead a frequency range. This causes spectral overlap for the two elements that make up equation 25. Making it impossible to distinguish between the amplitude modulation caused by the photoacoustic effect and the frequency modulation caused by the thermoelastic expansion using the data analysis that is part of the mDPA method.

3.5.1.2 Effect of non-linear acoustics on the mDPA effect

Besides the photoacoustic pulse that was ignored in the original experiment another physical parameter was neglected, namely the non-linear behaviour of acoustic waves. The acoustic waves can only be approximated to behave according to the linear wave equation as provided in 2.1, as long as the compression the wave undergoes is negligible[31]. All analysis and theory so far has been based on a linear approximation of the acoustic wave equation. Therefore for the results obtained in the experiments so far to be interpretable using the theory of linear acoustics, it has to be proven this is a reasonable assumption. This can be done through a measurement of the photoacoustic pressure amplitude. For this measurement a calibrated hydrophone needle can be used at a well-defined distance to the source. By using equation 2 in 2.1 an indication of the initial pressure of the photoacoustic signal can be obtained. If this pressure is in the linear regime then the conclusions made based on the measurement of both the mDPA effect and the PA signals can be assumed to hold. The value for the maximal pressure where the linear approximation is valid is based on figure 16 from Duck et al. where the regimes for acoustic wave propagation are described.

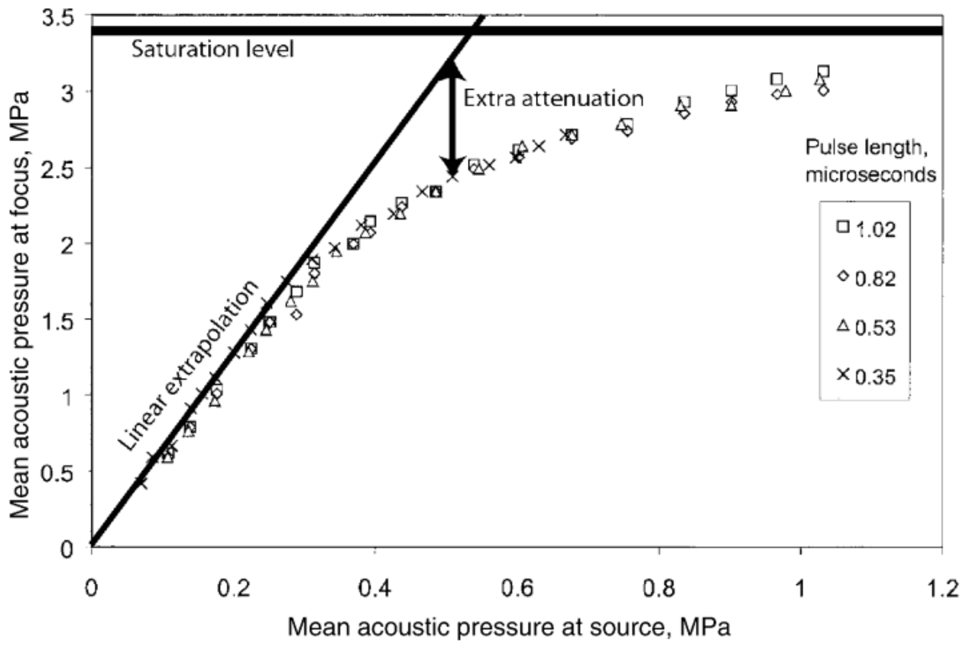

Figure 16 Figure by Duck et al. where the measurements were performed in water[31].

The maximal initial pressure where the linear approximation holds is taken to be 0.3 MPa or 300 kPa. Thus the pressure that is measured during the control experiment should be lower than 300 kPa.

3.5.2 Adjusted Data analysis

As a result of the negligible compression the following data analysis steps can be performed. We know from chapter 5 that the analysed data has the following expression:

$$mDPA_{filtered}(t) = \frac{1}{2}A_{US}A_R \sin[2\pi f_{mDPA})t] + \frac{1}{2}A_R A_{PA} \sin\left(2\pi\left(\sum f_{PA} - f_0\right)t\right)$$

(26)

For a PA measurement the signal outcome of the data analysis is

$$PA_{filtered}(t) = \frac{1}{2}A_R A_{PA} \sin\left(2\pi\left(\sum f_{PA} - f_0\right)t\right)$$

(27)

Then in the range where the compression can be neglected the PA result can be subtracted from the mDPA result to give.

$$mDPA_{filterednew}(t) = mDPA_{filtered}(t) - PA_{filtered}(t)$$

(28)

$$mDPA_{filterednew}(t) = \frac{1}{2}A_{US}A_R \sin[2\pi f_{mDPA}(t)t]$$

(29)

3.6 Preparing the experiments

3.6.1 positioning and alignment

Before performing the experiments to reproduce the mDPA effect. The set-up has to be properly prepared. This encompasses the positioning of the tube, and the alignment of the dual element transducer. For the positioning of the tube two blocks are present in the water tank that have a round hole in them. The placement is as described in figure 8. the tube is attached to the syringes using needles with a diameter of 0.50 mm. For the attachment of the tube, the tube is probed by tip of the needle and subsequently slowly rotated with as little pressure as possible to slide around the needle without puncturing the tube. This is then performed twice for both syringes.

The transducer alignment is done through translation in the z- and y- direction as in figure 17, by making use of translation stages.

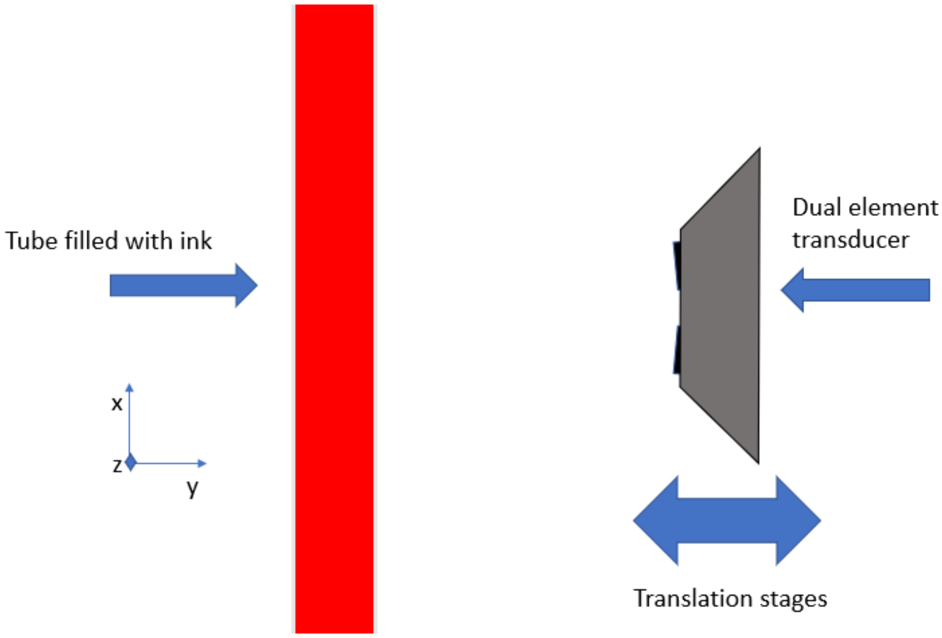

Figure 17 Top view of the placement of the dual element transducer.

For the alignment pulses are send by the send element of the dual element transducer and measured by the receive element. The received signal can be monitored on the oscilloscope where a local maximum is found in terms of signal amplitude. This local maximum can be determined through the translation of the stages in their respective directions and stopping at the position where any change of position leads to a decrease of signal amplitude. The distance to the tube at which this maximum occurs is at 33 mm for the transducer.

3.6.2 Preparation of the ink solution

The ink solution is prepared by first analyzing the absorption spectrum of the red ink to determine the dilution needed to have a 10 mm^{-1} ink solution. This is done by analysing a sample of the red ink which is diluted 1:50 $\frac{V}{V}$ in a spectrophotometer, to determine its absorption spectrum at the relevant wavelength of 532 nm. The full absorption spectrum is shown in figure 10.

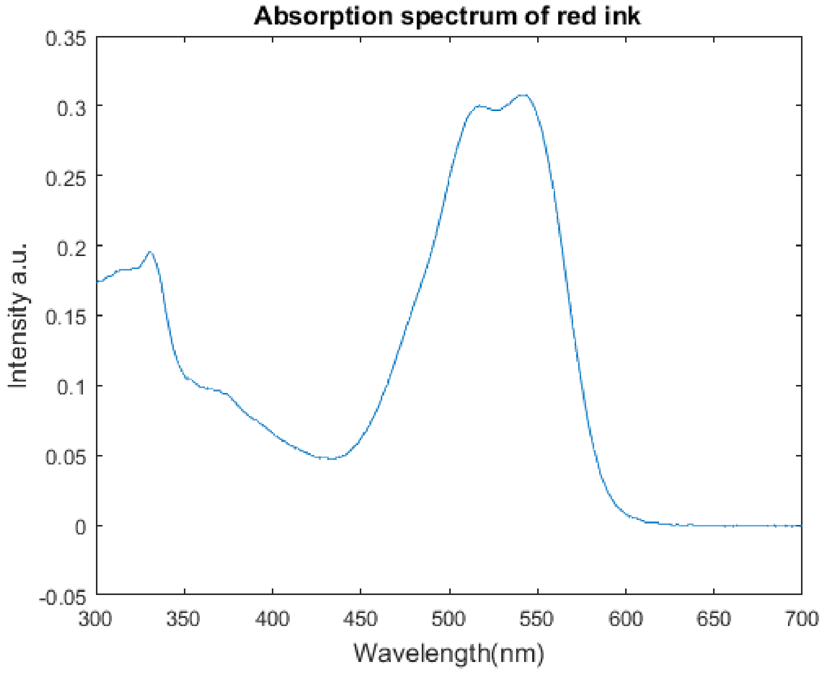

Figure 18 the absorption spectrum of the red ink solution with 1:50 $\frac{\mathrm{V}}{\mathrm{V}}$ dilution of the ink.

Using the results of the spectrophotometer the absorption at the wavelength of 532 nm was determined. Then this absorption can be implemented in equation 30.

$$\mu_{ext} = \frac{\ln(10^{Abs})}{d} = Abs\frac{\ln(10)}{d} \tag{30}$$

Where μ_{ext} is the extinction coefficient of the solution in mm^{-1}, Abs is the absorption measured by the spectrophotometer, and d is thickness of the cuvette that was used in mm. based on the values as shown in the figure the dilution was determined to be 1:60 $\frac{\mathrm{V}}{\mathrm{V}}$ i.e. 1 part ink and 60 parts demineralized water.

Chapter 4. Experimental results

4.1 Introduction

The results that are shown in this chapter are in order of relevance to the totality of the project. First the set-up that is used needs to be adequate and all conditions and working requirements have to be addressed before the final experiments obtain their value.

4.2 System validation

4.2.1 Lock in amplifier

The result shown in figure 19 is of two trial waves one that has frequency of 5MHz and duration of 3 µs and one that has frequency of 5.1 MHz and duration of 3 µs with a reference signal of 5 MHz. The output of the lock-in amplifier has a non-distinct result for these two trial waves shows that on this short time duration of a signal there is very little use for the lock-in amplifier.

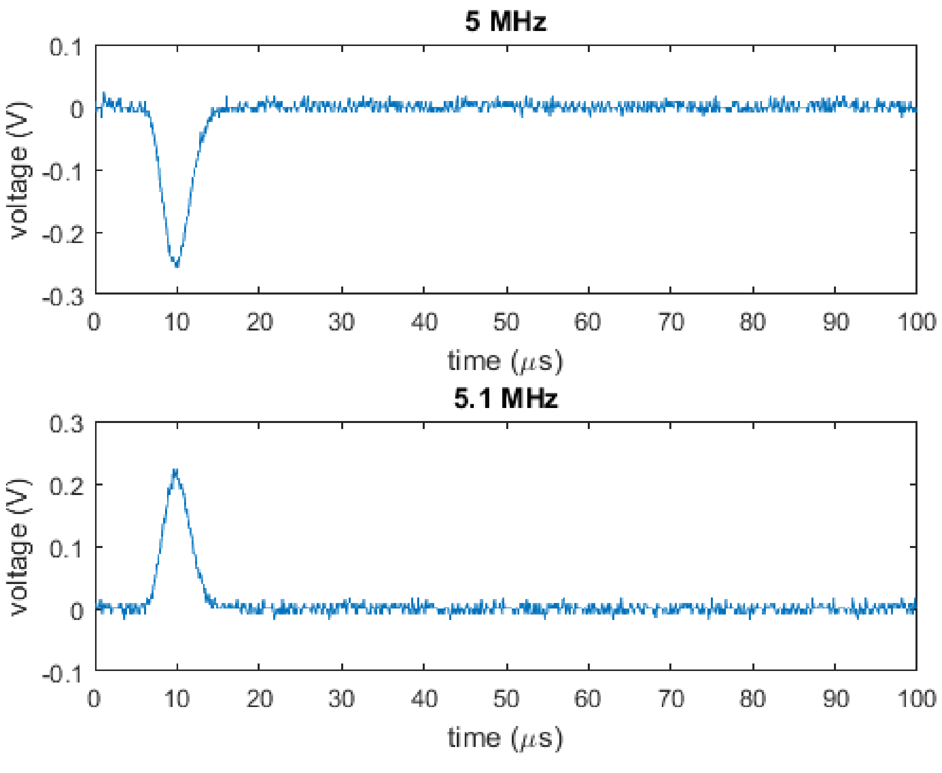

Figure 19 Output of lock-in amplifier for different trial waves.

This result shows that the use of the lock-in amplifier leads to problems in the data analysis as the lock-in amplifier does not give an output that is recognizable as a result that is expected based on the data analysis procedure.

4.2.2 Without lock-in amplifier

To test the functionality of the digital data analysis the same trial waves were used to see the response of the new data analysis. These results are shown in figure 20.

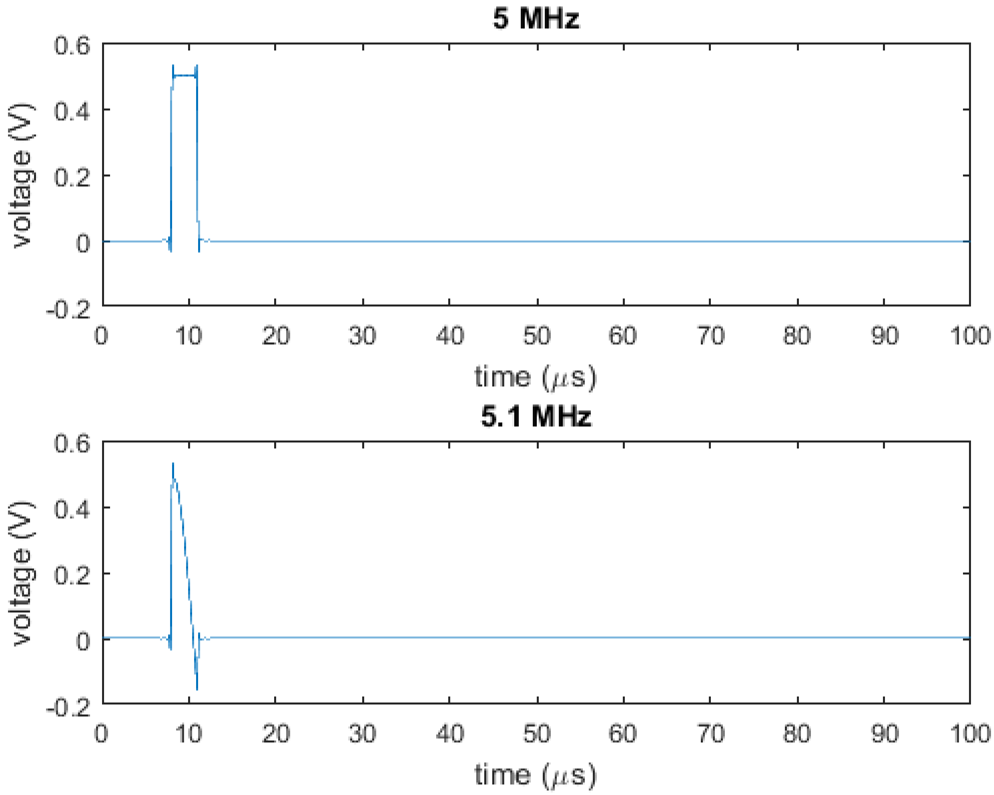

Figure 20. Result of digital implementation of the data analysis.

In this figure it is clearly visible that a difference in signal for both trial waves occurs. These results are more in agreement with the expectation of the data analysis as was shown in chapter 2.

4.2.3 Pressures of the photoacoustic pulses

Using this set up the calibration of the PA signal are performed for both the tube filled with water and red ink and the tube filled with ethanol and red ink, i.e. the set up explained in chapter 3. The pulse energies that are used are 5, 10, and 15 mJ per pulse with the same set up as for the mDPA measurement i.e. the positioning of the laser fiber and the tube is consistent across all the measurements.

The results of the measurements for ethanol with pulse energies 5 and 10 mJ and for water at 5 mJ pulse energy are shown in figure 21.

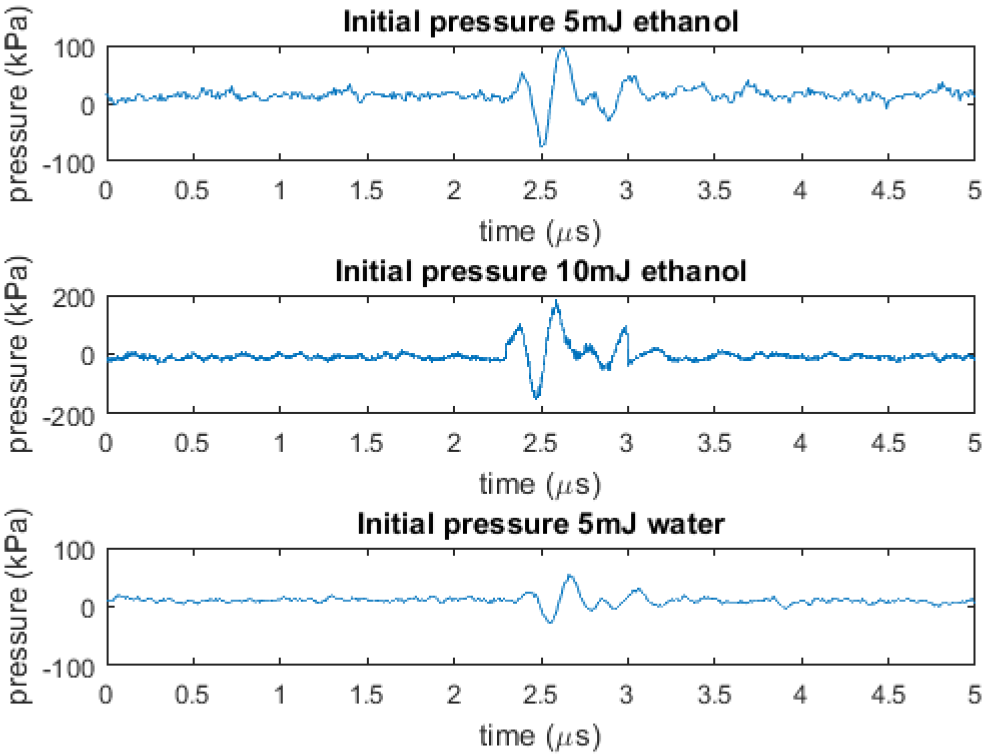

Figure 21. Initial pressure changes for the different set up configurations. Where t=0 indicates the start of data acquisition..

Based on these measurements it can be concluded that for all three of these measurements the maximal pressure that is measured is within the region where the linear approximation holds so in that condition both of the configurations are allowed. For the second part of the calibration measurement the induced Doppler shift has to be calculated. To do this equation 31 can be used.

$$\Delta f = 2\frac{\kappa R}{c_s}\frac{\partial p_{max}(t)}{\partial t}100 \tag{31}$$

Where Δf is the percentage of the frequency of the carrier wave. Then using the results obtained using the calibration measurement the maximal pressure derivative can be found. Using this method the expected values for the created Doppler shifts can be calculated. For water with red ink this results in $\Delta f = 0.11\%$ and for ethanol with red ink this results in $\Delta f = 0.5\%$.

4.2.4 Limits of experimental set-up

The limitations of the set-up are the constraints that define when the assumptions that are made in the steps of the data analysis hold, the ability of the measurement apparatus to detect signals and the characteristics of the phantoms. Based on these limitations the

exepriments that are of interest for both the micro-Doppler acoustics and micro-Doppler photoacoustics have the following properties.
The oscilloscope is an 8-bit oscilloscope which causes it to be unable to detect vertical differences smaller than 0.39%. Because of the values that were obtained in the previous paragraph the mDPA experiment with water is not expected to give any results. Ethanol should give a measurable doppler shift.

Based on chapter 3 it is known that for pressures up to 300 kPa the non-linearity of the signals can be ignored, for ethanol at 5 mJ pulse the maximal pressure was roughly ≈200 kPa. Thus the non-linearity for ethanol is negligible. Based on the requirements that were determined to be necessary for the detection of the mDPA effect, the optimal set up for the final mDPA measurements is to use ethanol with red ink as the absorber and work with pulse energies of 5 and 10 mJ.

4.3 Results of the micro-Doppler acoustics experiments

After performing the experiment and applying the appropriate data analysis the experimental results of this experiment are obtained. Two experiments with different input voltages for the reflection transducer are represented to show the results are consistent. The effect on the piezo of the reflection transducer should be roughly linear with voltage within the operating range of the piezo. In this experiment the expected amplitude of movement is in order of magnitude of 1 µm. These results are shown in figure 21.

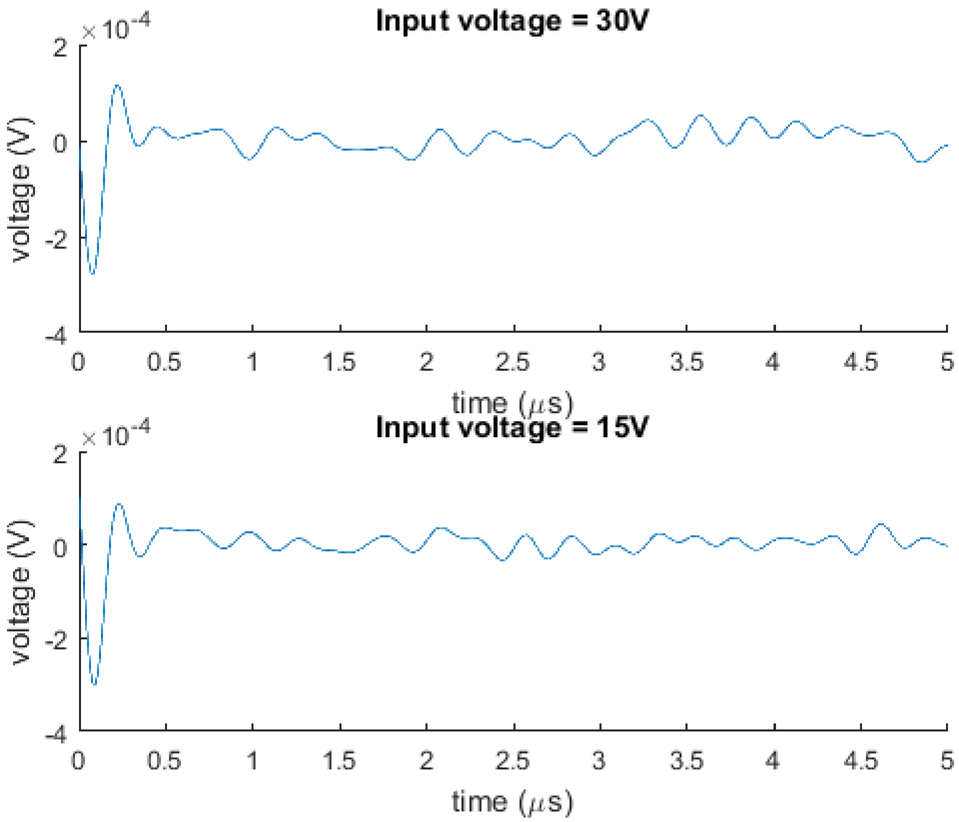

Figure 22. Result of the micro-Doppler experiment for two voltages.

What is obvious when doing the comparison between the static Doppler model and the experimental results something unforeseen has happened. As there are no harmonic elements contained within the frequency/amplitude modulation of the carrier wave something in the experiment has failed. As even for the case where the model should be changed to be based on the quasistatic Doppler there should be a set of harmonics in the analysed data. Using the fact that the measurements were done with multiple amplitudes of the oscillation of the vibrating surface certain conclusions can be made. The first is the lack of harmonics shows the quasistatic Doppler effect is not the cause for the signal that can be detected using the mDPA method, as that should give at least some 0.5 MHz harmonics in the analysed data. Second is the possibility of inferior measurement instruments. After some research into the possible limiting factors of the system the main issue was proven to be the low resolution of the oscilloscope as mentioned in the limitation of the set-up. This means that the frequency difference that can be detected on the timescales where the measurement were performed, must at least be 0.39% of the carrier frequency. This is also corroborating information for the fact that the quasistatic Doppler effect does not have an influence on the measurements, as that effect is measurable using the set up but the amplitude of the reflection transducer is limited and only gives a Doppler shift of 0.13%.

4.4 Results of mDPA measurements

4.4.1 Reproducing F.Gao et al.

The first step that is taken in assessing the effect of the mDPA effect on the ultrasound signal is to see if the experiments that are done give the results that are expected based on the results obtained by F. Gao et al. The steps of the data analysis that was used for the results are shown in figure 23 where the green line indicates the moment in time in the received signal where the laser pulse occurs. First the mDPA and PA signals are measured, then the signals are mixed and finally filtered.

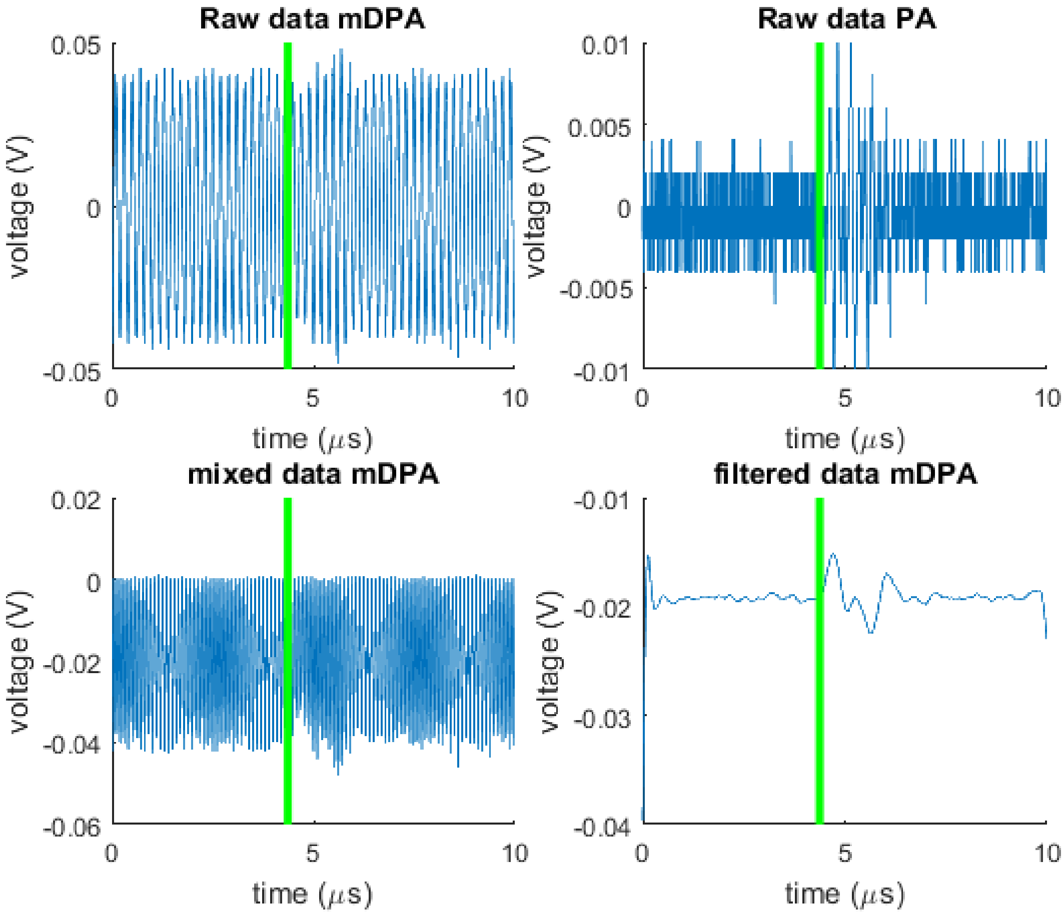

Figure 23: Results from mDPA experiments through the stages of data analysis to the result of interest. Results given are obtained from measurement at a laser energy of 5 mJ.

The final result of the data processing looks like the signal as is described by Gao et al.[15] this indicates that the replication of the mDPA effect seems to have been successful, or at the very least the result of the experiment that is performed corresponds to the result of the experiment that is being reproduced.

4.4.2 Effect of PA signal

The reassessment of the theory indicates there is not just frequency modulation but also amplitude modulation. Therefore it was decided to test if the result of the PA signal also gives a result that looks like the filtered data of figure 23. So the data analysis was also applied to the raw PA data, that was captured by the receiving element while the send element was turned off. The comparison between both of these results is visible in figure 24.

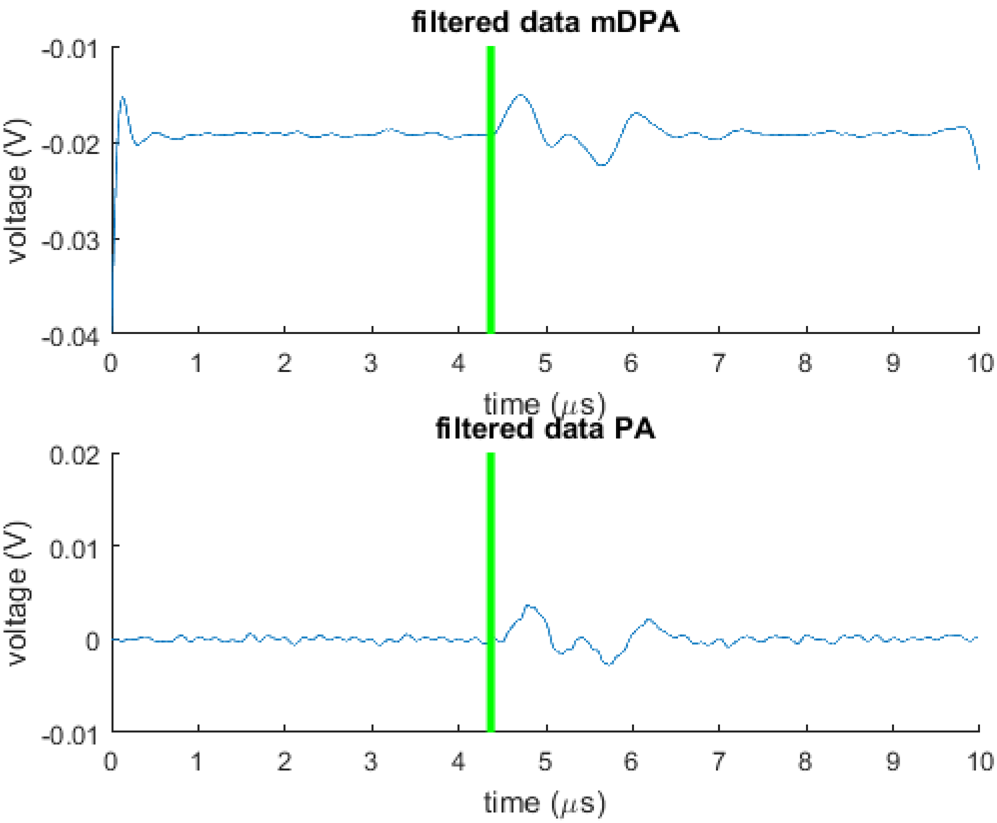

Figure 24: comparison between the filtered mDPA results and filtered PA results. Results given are obtained from measurement at a laser pulse energy of 5 mJ.

The comparison shown in figure 24 indicates that a large part of the signal modulation that occurs during the measurement of the mDPA effect is due to the amplitude modulation given by the PA pulse. The difference in the baseline voltage between both graphs is the result of the phase which is neglected in the data analysis but does show up in the eventual results.

4.4.3 Revised mDPA procedure

The experiments that have been performed until now have given the knowledge that the only experiments that should give a measurable effect that is entirely attributable to FM. For ethanol at 5 mJ laser pulse energy this result is given in figure 25. This is the result of averaging 100 times to reduce the noise and give a better picture into the mechanics of the process, it also reduces the effect of laser pulse variability.

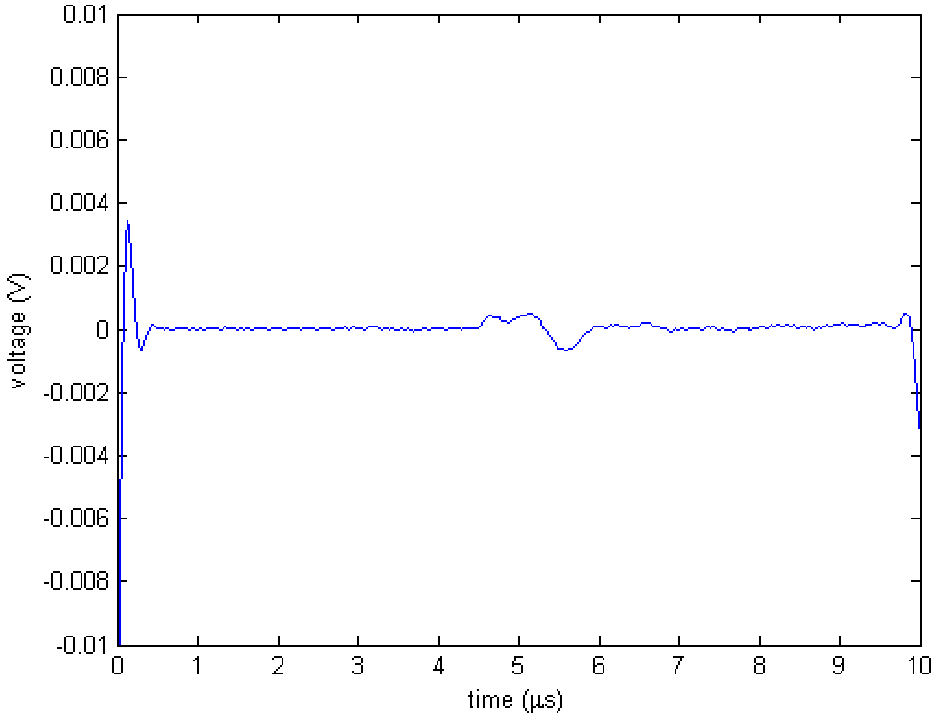

Figure 25. FM signal based on mDPA effect for 5 mJ pulse energy, for ethanol with red ink.

The maximal pressure for a pulse energy of 10 mJ per pulse was measured to be ≈ 290kPa, so the measurement is at the edge of the regime where the assumption holds. The result for 10 mJ is in figure 26.

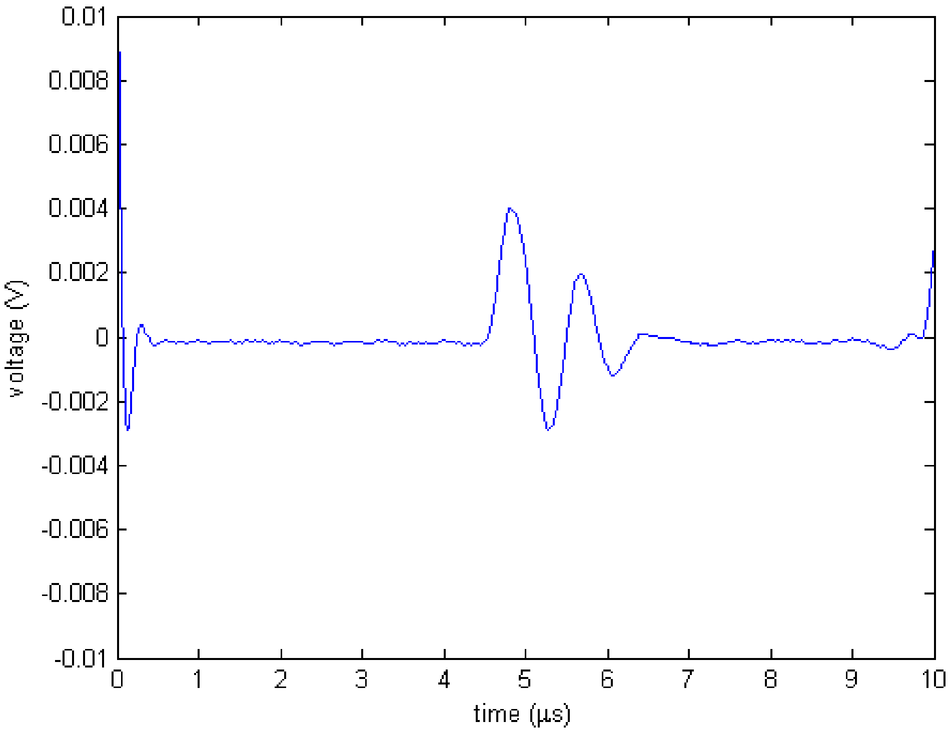

Figure 26. FM signal based on mDPA effect for 10 mJ pulse energy, for ethanol with red ink.

Based on the results of figure 25 and 26 there appears to be a small FM signal as a result of the mDPA effect. But when looking at the increase in magnitude of the strength of the FM signal this is much more than a linear increase of the strength where this should be lower or equal based on equation 12. A possible explanation of this is the fact that small doppler shifts don't show up in the measurements because they can't be resolved by the oscilloscope. In that sense for the 5 mJ pulse energy only a fifth of the maximal doppler shift is above the resolution limit, while the 10 mJ pulse energy has $\Delta f = 1.0\%$ so 60% of the maximal doppler shift is above the resolution limit. The effect is that the section of signal that contributes to the deviation from is significantly larger for the 10 mJ pulse. This might be part of the cause for the significant increase in strength between both measurements. The other possibility is that for 290 kPa the pressure is too high causing compression of the acoustic waves.

4.5 Conclusion

The results that were obtained during this thesis, the important results were shown in this chapter, allow for an assessment to be made with regards to validity of the results that were obtained. Based on the validations of the set-ups the requirements that are necessary to perform the new data analysis were proven to be met. The limitation of the oscilloscope is the biggest hurdle to make any hard statements about the possibility of FM signal creation using the photoacoustic effect. The results of figure 25 does seem to indicate the existence of the FM signal but there is still the doubt that is raised due to the non-linear increase in signal strength between figure 25 and 26. But that could be resolved using a 14- or 16-bit oscilloscope. From figure 24 it can also be concluded that there is no significant increase in signal quality as a result of the mDPA effect as described by F. Gao et al. There is a small increase but the quality improvement does not match up to the claims in that paper.

Chapter 5. Conclusion and outlook

5.1 Reflections on the experimental results

At the start of this thesis the goal was to investigate the possibility of using FM to first measure photoacoustic signals in the hopes of being able to use this in increasing the imaging depth of PAT for breast imaging. This was done through first testing the claims of F. Gao et al. in their paper on the mDPA effect where the photo-elastic expansion induces a frequency modulation on the carrier wave of the ultrasound radar system. It turns out that the assumptions and data analysis that were proposed by F. Gao et al. were incomplete. First of all it is necessary to account for the photoacoustic pulse. Since the Pa signal also reaches the receive transducer and that creates an amplitude modulation in the signal. Because this first assumption doesn't hold up the data analysis has to be adjusted to account for the PA signal.

To be able to confidently make the statement that it is possible to create FM signals in ultrasound by photo-elastic expansion through laser light illumination, it needs to be possible to directly compare the effect of the PA signal and the effect of the mDPA effect where these two elements are distinguishable. This causes some problems as it not possible to subtract the signals if the pressure is too high. When the pressures that are produced in the system are too high the signals are not subtractable as is needed for the analysis of the expanded mDPA model. Also there is the problem of the limited timescale where signal modulation occurs, because of the uncertainty principle the frequency elements that are present in either the mDPA or the PA signal can not all be distinguished using conventional fourier analysis. So only in the regime where the assumptions and approximations of the expanded mDPA effect the existence of frequency modulation in the ultrasound radar signal can be examined.

Based on the results that were obtained after going through the correct steps i.e. the results shown in 4.4.3. The assesment can be made that FM does in fact occur through the photo-elastic expansion induced by laser light illumination. Based on the initial motivation of using the mDPA effect to improve the SNR of PAT and improve imaging depth, there are numerous problems. The actual mDPA effect actually needs a lot of averaging to be raised above the noise floor as is seen in 4.4.3 where the final results are averaged a 100 times. So the improvement in signal quality is not actually produced using FM on ultrasound. At most using FM on ultrasound can slightly improve the quality of the signal in PAT using the combination of the photoacoustic signal and the frequency modulation to marginally improve the signal quality.

5.2 Conclusion

The conclusion that there is a slight improvement possible using the mDPA effect does actually correspond to the claims made by Gao et al. The physics of the mDPA effect has been expanded on in this thesis where the model for the mDPA effect was improved to give physically sound predictions in the case of linear approximation for the acoustic propagation in the system. Also the problem with trying to increase imaging depth of PAT using this method is that the Doppler shifts that are induced in deeper tissue are much smaller than in superficial tissue and can be so small that they are of a similar order of magnitude as the Doppler shifts that are induced by movements in the body, such as a heartbeat or blood flow.

5.3 Outlook

The implementation of FM signal creation on ultrasound in PAT is possible. It should even give a slight improvement in the SNR of the measurements. The problems that are introduced by expanding a PAT system to include FM, are in practice much more than the minor improvement in signal quality. Therefore any additional research into improving the SNR and imaging depth of PAT should be done in other directions as FM signal creation in ultrasound has been a futile exercise for trying to improve these elements of PAT.

It would be interesting to use a better oscilloscope i.e. 14-or 16-bit to redo the acoustic and photoacoustic Doppler effect measurements to see if the conclusions that were made in this thesis do in fact hold up or if some mistakes were made.

References

1. Evaluate, *Global top 10 companies based on diagnostic imaging market share in 2016 and 2022*, Statista, https://www.statista.com/statistics/331739/top-global-companies-by-diagnostic-imaging-market-share/. (2017)
2. Mangan D*., Medical Bills Are the Biggest Cause of US Bankruptcies: Study*, CNBC, 24 july 2013, https://www.cnbc.com/id/100840148.
3. Hovenkamp H. J., *Whatever Did Happen to Antitrust Movement?*, University of Pennsylvania Law School Institute for Law and Economics Research Paper, (2018).
4. Orbach B., *How Antitrust Lost Its Goal*, 81 Fordham L. Rev. 2253 (2013)
5. Xia J, Yao J, and Wang L.V., *Photoacoustic tomography: principles and advances*. Electromagn Waves (Camb). 147, 1-22. (2014)
6. Yao J, Wang L.V., *Photoacoustic tomography: fundamentals, advances and prospects*. Contrast Media Mol Imaging. 6(5), 332-45. (2011).
7. Dhawan A.P., D'Alessandro B., and Xiaolei F., *Optical imaging modalities for biomedical applications*, IEEE Rev. Biomed. Eng., vol. 3, pp. 69–92, (2010).
8. Heijblom, M. et al. *Photoacoustic image patterns of breast carcinoma and comparisons with Magnetic Resonance Imaging and vascular stained histopathology*. Sci. Rep. 5, 11778; doi: 10.1038/srep11778 (2015).
9. Jemal, A. et al. Global cancer statistics. CA Cancer J. Clin. 61, 69–90 (2011).
10. Geroski P.A., Machin S, Reenen J.V.. *The Profitability of Innovating Firms*. The RAND Journal of Economics, Vol. 24, No.2: 198-211. (1993).
11. Geroski, P.A., and R.Pomroy. *Innovation and the Evolution of Market Structure*. The Journal of Industrial Economics, Vol. 38, No.3: 219-314. (1990).
12. Aghion P., Bechtold S., Cassar L., and Herz H., *The causal effects of competition on innovation: Experimental evidence*. Working Paper, (2014).
13. Favazza C., Maslov K., Cornelius L., Wang L. *In vivo functional human imaging using photoacoustic microscopy: response to ischemic and thermal stimuli,* Proc. SPIE 7564, Photons Plus Ultrasound: Imaging and Sensing 2010, 75640Z (2010);
14. Hagen J.B., *Radio-Frequency Electronics: Circuits and Applications*, 2009, Cambridge University press.
15. F. Gao, X. Feng, and Y. Zheng, *Micro-Doppler Photoacoustic Effect and Sensing by Ultrasound Radar,* IEEE Journal of Selected Topics in Quantum Electronics, vol. 22, no. 3, pp. 1-6, (2016).
16. Kinsler L.E., Frey A.R., Coppens A.B., and Sanders J.V., *Fundamentals of Acoustics, 4th Edition,* 1999, Hoboken, Wiley & sons.
17. Lurton X., *An Introduction to Underwater Acoustics ch.2*, 2010, Berlin, Springer-Verlag.
18. Blackstock, D. T. ,*Fundamentals of Physical Acoustics,* 2000, New York, John Wiley & Sons.
19. Szabo T., *Diagnostic Ultrasound Imaging: Inside Out*, 2004, London, Elsevier.
20. A. G. Bell, *On the production and reproduction of sound by light*, Am. J. Sci. 118, 305–324 (1880).
21. M. L. Veingerov*, A method of gas analysis based on the Tyndall-Röntgen optico-acoustic effect*, Dokl. Akad. Nauk SSSR 19, 687–688 (1938).

22. Wang X., Pang Y., Ku G., Xie X., Stoica G., and Wang LV., *Noninvasive laser-induced photoacoustic tomography for structural and functional in vivo imaging of the brain,* Nat Biotech. 21, 803–806. (2003).
23. Wang L.V., *Tutorial on Photoacoustic Microscopy and Computed Tomography. Selected Topics in Quantum Electronics*, IEEE Journal of. 14, 171–179 (2008).
24. S. L. Jacques, *Role of tissue optics and pulse duration on tissue effects during high-power laser irradiation,* Appl. Opt. 32, 2447–2454 (1993).
25. A. Karabutov, N. B. Podymova, and V. S. Letokhov, *Time-resolved laser optoacoustic tomography of inhomogeneous media*, Appl. Phys. B 63, 545–563 (1996).
26. V. E. Gusev and A. A. Karabutov, *Laser Optoacoustics,* American Institute of Physics, (1993).
27. Yong Zhou, Junjie Yao, and Lihong V. Wang, *Tutorial on photoacoustic tomography,* J. Biomed. Opt. 21(6) 061007 (2016).
28. Wang L.V., *Photoacoustic Imaging and Spectroscopy*, 2009, Boca Raton, CRC Press.
29. R. Wunenburger, N. Mujica, and S. Fauve, *Experimental study of the Doppler shift generated by a vibrating scatterer,* Journal of the Acoustical Society of America, vol. 115, pp. 507-514, (2004).
30. V. C. Chen, F. Y. Li, S. S. Ho, and H. Wechsler, *Micro-doppler effect in radar: Phenomenon, model, and simulation study,* IEEE Transactions on Aerospace and Electronic Systems, vol. 42, pp. 2-21, (2006).
31. Duck, F. A. . *Nonlinear acoustics in diagnostic ultrasound*. Ultrasound in Med. & Biol. 28, 1–18. (2002).

Appendix A

The matlab script that was used to read out the data from the oscilloscope, is given below.

```
k=1; % Input definition used for starting the loop.

% Create a VISA-USB object.
interfaceObj = instrfind('Type', 'visa-usb', 'RsrcName',
'USB0::0x0699::0x03A6::C018440::0::INSTR', 'Tag', '');

% Create the VISA-USB object if it does not exist
% otherwise use the object that was found.
if isempty(interfaceObj)
    interfaceObj = visa('TEK',
'USB0::0x0699::0x03A6::C018440::0::INSTR');
else
    fclose(interfaceObj);
    interfaceObj = interfaceObj(1);
end

% Create a device object.
deviceObj = icdevice('tektronix_tds2024.mdd', interfaceObj);

% Connect device object to hardware.
connect(deviceObj);
% Create loop for the number of times the waveform is read
out.
for k=1:100

groupObj = get(deviceObj, 'Waveform');
groupObj = groupObj(1);
[Y, X] = invoke(groupObj, 'readwaveform', 'channel1');
% Storing of the multiple waveforms in conjunction.
if k==1
xmdpa60mV3mjeth4((k-1)*2500+1:2500*k)=X(:);
ymdpa60mV3mjeth4((k-1)*2500+1:2500*k)=Y(:);
k=k+1;
else
xmdpa60mV3mjeth4((k-
1)*2500+1:2500*k)=X(:)+xmdpa60mV3mjeth4((k-1)*2500)-
xmdpa60mV3mjeth4(1);
ymdpa60mV3mjeth4((k-1)*2500+1:2500*k)=Y(:);
k=k+1
end
```

```
end
```